# First observation of isomeric states in $^{111}$Zr, $^{113}$Nb, and $^{115}$Mo

J. Wu,[1,*] S. Nishimura,[2] P.-A. Söderström,[3] A. Algora,[4,5] J. J. Liu,[2,6] V. H. Phong,[2] Y. Q. Wu,[7] F. R. Xu,[7] J. Agramunt,[4] D. S. Ahn,[2] T. A. Berry,[8] C. G. Bruno,[9] J. J. Bundgaard,[10] R. Caballero-Folch,[11] A. C. Dai,[7] T. Davinson,[9] I. Dillmann,[11] A. Estrade,[12] A. Fijałkowska,[13,14] N. Fukuda,[2] S. Go,[2] R. K. Grzywacz,[10,15] T. Isobe,[2] S. Kubono,[2] G. Lorusso,[2,8,16] K. Matsui,[2,17] A. I. Morales,[4] N. Nepal,[12] S. E. A. Orrigo,[4] B. C. Rasco,[15] K. P. Rykaczewski,[15] H. Sakurai,[2] Y. Shimizu,[2] D. W. Stracener,[15] T. Sumikama,[2] H. Suzuki,[2] J. L. Tain,[4] H. Takeda,[2] A. Tarifeño-Saldivia,[4,18] A. Tolosa-Delgado,[4] M. Wolińska-Cichocka,[19] and R. Yokoyama[10]

[1]*National Nuclear Data Center, Brookhaven National Laboratory, Upton, New York 11973, USA*
[2]*RIKEN Nishina Center, 2-1 Hirosawa, Wako-shi, 351-0198 Saitama, Japan*
[3]*Extreme Light Infrastructure – Nuclear Physics (ELI-NP), Bucharest-Magurele 077125, Romania*
[4]*Instituto de Física Corpuscular (CSIC-Universitat de Valencia), Apartado Correos, 22085, E-46071 Valencia, Spain*
[5]*Institute of Nuclear Research, ATOMKI, 4026 Debrecen, Hungary*
[6]*Department of Physics, University of Hong Kong, Pokfulam Road, Hong Kong*
[7]*School of Physics and State Key Laboratory of Nuclear Physics and Technology, Peking University, Beijing 100871, China*
[8]*Department of Physics, University of Surrey, Guildford GU2 7XH, United Kingdom*
[9]*School of Physics and Astronomy, University of Edinburgh, Edinburgh EH9 3FD, United Kingdom*
[10]*Department of Physics and Astronomy, University of Tennessee, Knoxville, Tennessee 37996, USA*
[11]*TRIUMF, Vancouver, British Columbia, Canada V6T 2A3*
[12]*Department of Physics and Science of Advanced Materials Program, Central Michigan University, Mount Pleasant, Michigan 48859, USA*
[13]*Department of Physics and Astronomy, Rutgers University, New Brunswick, New Jersey 08854, USA*
[14]*Faculty of Physics, University of Warsaw, Warsaw PL-02-093, Poland*
[15]*Physics Division, Oak Ridge National Laboratory, Oak Ridge, Tennessee 37830, USA*
[16]*Chemical Medical and Environmental Science Division, National Physical Laboratory, Teddington TW110LW, United Kingdom*
[17]*Department of Physics, University of Tokyo, Hongo 7-3-1, Bunkyo-ku, 113-0033 Tokyo, Japan*
[18]*INTE-ETSEIB, Universitat Politecnica de Catalunya (UPC), E-08028 Barcelona, Spain*
[19]*Heavy Ion Laboratory, University of Warsaw, Ludwika Pasteura 5A, 02-093 Warszawa, Poland*

(Received 22 October 2022; revised 28 November 2022; accepted 8 December 2022; published 26 December 2022)

Isomeric states in the neutron-rich nuclei $^{111}$Zr [$T_{1/2} = 0.10(7)$ μs], $^{113}$Nb [$T_{1/2} = 0.7(4)$ μs], $^{115}$Mo [$T_{1/2} = 46(3)$ μs] were first identified at the Radioactive Ion Beam Factory (RIBF) of RIKEN by using in-flight fission and fragmentation of a $^{238}$U beam at an energy of 345 MeV/u. This is a brief report of the $\gamma$ transitions deexciting from isomeric states and half-lives measurements, which provides the first spectroscopy in the nuclear region of prolate-to-oblate shape-phase transition around mass A ≈110.

DOI: 10.1103/PhysRevC.106.064328

## I. INTRODUCTION

Atomic nuclei consisting of protons and neutrons reflect various kinds of shapes in nature. The existence of “magic numbers” of nucleons at 8, 20, 50, 82 was first pointed out by Goeppert-Mayer and entirely explained after introducing a harmonic oscillator potential with the spin-orbital interaction [1]. The nuclei with doubly “magic” numbers of protons and neutrons exhibits a spherical shape and start deforming when removing or adding protons and neutrons, which is manifest by the occurrence of shape-phase transition driven by the proton-neutron interaction.

The sudden onset of deformation beyond neutron number $N = 60$, first discovered at $_{40}$Zr by Johansson [2], was observed and interpreted with a strong tensor force between proton $\pi g_{9/2}$ and neutron $\nu g_{7/2}$ induced by the increased occupation of the $\nu g_{7/2}$ orbital [3–5]. From thereon, a large degree of connectivity and ground-state quadrupole deformation is manifest toward the middle shell between $N = 50$ and $N = 82$ major closed shells [6,7]. The maximum deformations of the ground state are achieved at $N = 64$ and $N = 62$ for the neutron-rich $_{42}$Mo and $_{40}$Zr isotopes [8,9], respectively, followed by a well-known region of $Z \approx 40$ and $N \approx 72$ in the nuclear chart with a predicted shape phase transition and shape coexistence between prolate, triaxial, and oblate [10]. The finite-range liquid-drop model (FRDM) with Bardeen-Cooper-Schrieffer methods indicated the prolate-to-oblate shape phase transition occurs at $N = 74$, 73, 72 for $_{40}$Zr, $_{41}$Nb, $_{42}$Mo isotopes, respectively [11]. The covariant density functional theory (CDFT) with density-dependent point-coupling parameters, and the Hartree-Fock-Bogoliubov (HFB) calculations with D1S-Gogny interaction, predicted

*Corresponding author: jwu2@bnl.gov

 

a gradual shape-phase transition from $\gamma$-soft rotor at $^{100}$Mo ($N = 58$) to well-deformed oblate shape at $^{110}$Mo ($N = 68$) [12,13]. On the experimental side, the ground state of $^{110}$Zr was suggested to be a well-deformed shape [14–16], contradicting a predicted doubly magic spherical nuclei and the existence of a $N = 70$ subshell gap [17]. The energy and lifetime measurements of low-lying excited states in $^{100-110}$Zr did not show any signature of oblate structures in the $_{40}$Zr isotopes [6,8]. The flat pattern of $(\Delta E_J\text{-}\Delta E_{J-1})/\mathrm{E}(2_1^+)$ observed in $^{110}$Mo suggests its $\gamma$ vibrational feature, inconsistent with the previously suggested $\gamma$-soft rotor [9,18]. There is no experimental signature of oblate shape and $\gamma$-soft rotor observed in the $_{42}$Mo isotopes.

Detailed nuclear structure information in the neutron-rich $A \approx 110$ region has potential implications on the understanding the rapid ($r$-) neutron capture process [19]. Traditional main $r$-process nucleosynthesis is not capable of reproducing the observed abundance around the mass $A \approx 110$ region. A new nucleosynthesis mechanism named "weak $r$ process" is introduced for the compensation [20]. The spectroscopic information in the mass $A \approx 100$ region is extremely rare due to lots of hard-overcome difficulties in the isotope productions. Recent developments of new-generation radioactive beam accelerator systems employing the production mechanisms of in-flight fission and fragmentation provide an opportunity to access the first spectroscopic information in this region. Study of the low-lying excited states in the neutron-rich $A \approx 110$ nuclei will serve as a benchmark for testing theoretical calculation and helps better understand the contributions of main and weak $r$-process nucleosynthesis.

In the present work, we briefly report the identification of isomeric states in $^{111}$Zr, $^{113}$Nb, $^{115}$Mo, which will provide guidance for future studies with the development of rare isotope facilities.

## II. EXPERIMENT

The neutron-rich isotopes $^{111}$Zr, $^{113}$Nb, $^{115}$Mo were produced by a 345-MeV/u $^{238}$U primary beam with an intensity of ~30 pnA impinging on a 4-mm $^{9}$Be target at the Radioactive Isotope Beam Factory (RIBF). The projectile fission fragments were selected and identified by the large-acceptance BigRIPS and ZeroDegree spectrometers. Separation and identification of the cocktail secondary beam were conducted based on the TOF-B$\rho$-$\Delta$E principle by employing the radiation detectors along the beam line (see Fig. 1) [21]. The isotopes of interest were finally implanted in the beta counting system with a rate of ~30 pps, which consists of four double sided silicon strip detectors (DSSSDs) and one segmented YSO (yttrium orthosilicate, $Y_2SiO_5$) detector surrounded by 140 proportional counters filled with $^{3}$He gas and two HPGe clover-type detectors embedded in a high-density polyethylene moderator [22–25]. The emitted prompt and $\beta$-delayed $\gamma$ rays were detected with a full-energy peak $\gamma$ detection efficiency of 1.93(5)% at 1 MeV calibrated with the $^{133}$Ba and $^{152}$Eu sources [26–28]. The present work is part of the BRIKEN campaign, which is an international collaborative experimental program aiming to study the $\beta$-delayed neutron emission at RIKEN [29].

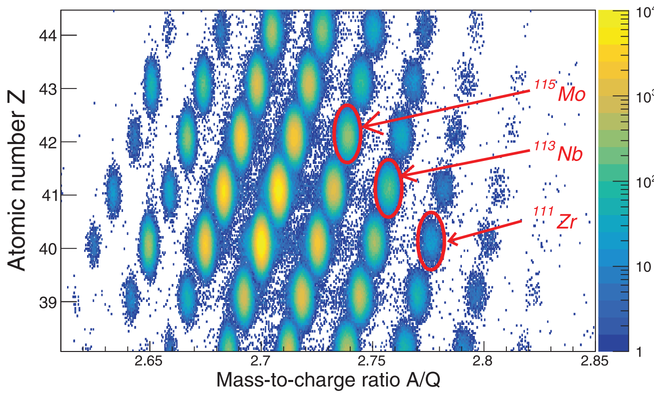


FIG. 1. Particle identification plot with atomic number (Z) vs mass-to-charge ratio constructed by the TOF-B$\rho$-$\Delta$E mechanism. The isotopes of $^{111}$Zr, $^{113}$Nb, $^{115}$Mo are tagged with red circles in this plot.

Data analysis was performed using conventional decay spectroscopy techniques after the identification of implanted ions on an event-by-event basis [19,30,31]. The prompt $\gamma$ rays are correlated with the heavy ions by the time-stamp information. The energy spectra of delayed $\gamma$ rays in $^{111}$Zr, $^{113}$Nb, and $^{115}$Mo are displayed in Fig. 2 with the identified transitions depopulating from the isomeric states. The exponential curves of isomeric decay obtained by applying the gates of delayed $\gamma$ rays are fitted with the unbinned maximum likelihood method to extract the half-lives. The reduced transition strength $B(\sigma\lambda)$ in $^{111}$Zr, $^{113}$Nb, $^{115}$Mo are extracted by assuming different multipolarities (see Table I) and taking into account the internal conversion coefficients calculated using BrIcc [32]. Excitation energies of the isomeric states in $^{111}$Zr, $^{113}$Nb, $^{115}$Mo are much lower than the energy needed to break a pair of protons and neutrons ($2\Delta_\pi = 2.5$ MeV and $2\Delta_\nu = 2.1$ MeV [33,34]), indicating their origins from single proton or neutron configurations.

## III. RESULTS AND DISCUSSION

Because of the limited information in these measurements, the spins and parities of levels, as well as their associated collective structures, cannot be well investigated. However, some key characteristic properties of the $\gamma$ transitions could be identified and indicated.

The isomeric state decaying to the ground state via a transition of 265 keV was observed in $^{111}$Zr, with an isomeric ratio estimated at 17(2)%. The half-life was measured to be a value of 0.10(7) µs by fitting the decay curve in coincidence with the 265-keV transition [see Fig. 2 (top)]. The calculated transition strengths when assuming various transition types (see Table I) ruled out $M2$ and higher-multipole transitions because their strengths exceed the recommended upper limit for each type of transition [35]. The small isomeric ratio indicates the higher spin of the isomeric state compared to that of the ground state, since the high-spin excited states are favored to be populated by the in-flight fission and fragmentation mechanism [36–38].

The isomeric state at 135 keV was first identified in $^{113}$Nb, with a half-life estimated at 0.7(4) µs [see Fig. 2 (middle)].

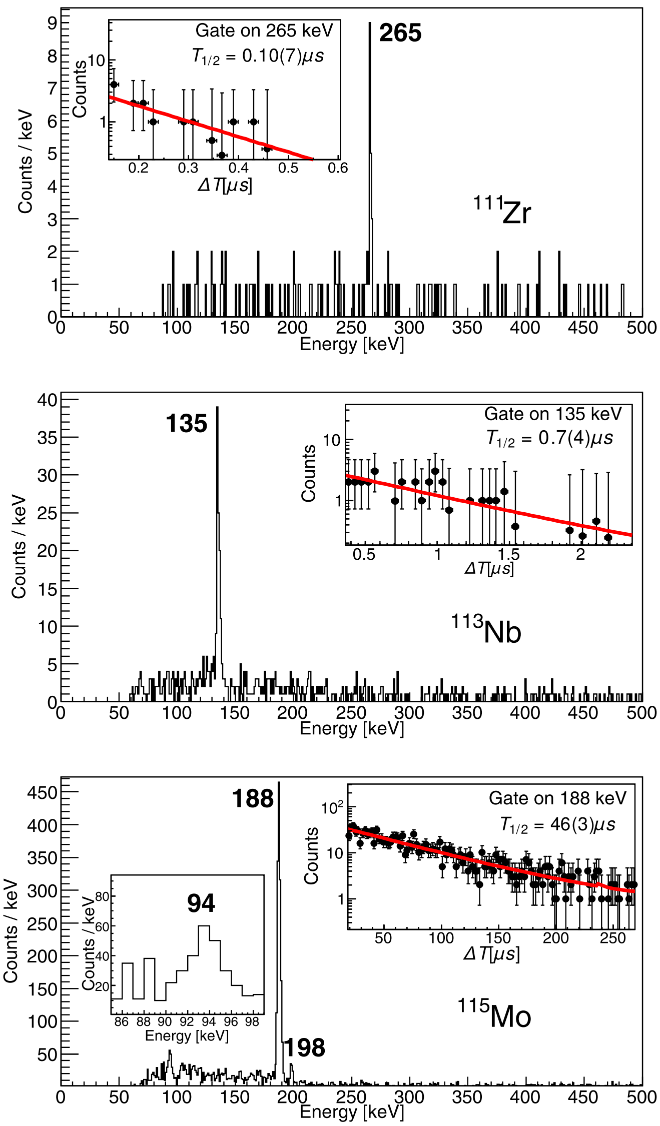


FIG. 2. Energy spectra of delayed $\gamma$ rays from $^{111}$Zr, $^{113}$Nb, $^{115}$Mo observed within 0.5 μs, 2.6 μs, 300 μs following implantation, respectively. (Inset) The exponential decay curves from the isomeric decay of $^{111}$Zr, $^{113}$Nb, $^{115}$Mo obtained by gating on the 265-keV, 135-keV, 188-keV transitions, respectively, as well as an energy spectrum of delayed $\gamma$ rays from $^{115}$Mo with a range of 85–99 keV. The half-lives of isomeric states were extracted by fitting the decay curve with the unbinned maximum likelihood method.

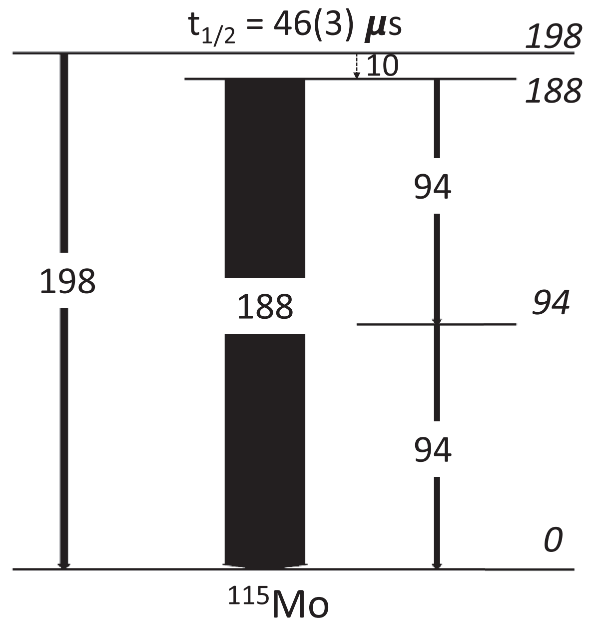


FIG. 3. Partial level scheme of $^{115}$Mo obtained in this work. The widths of arrows represent the relative intensities of $\gamma$ transitions. The dashed arrow shows the unobserved transition due to the small energy of 10 keV.

The isomeric ratio was determined to be 9(2)% by a ratio between the adopted level intensity and total implanted $^{113}$Nb events. The $M2$ and higher-multipole transitions were ruled out because their strengths exceed the recommended upper limit for each type of transition [35] (see Table I). The small isomeric ratio suggests that the spin of the isomeric state is larger than that of the ground state [36–38].

The isomeric state at 198 keV was first identified in $^{115}$Mo, with an isomeric ratio and a half-life estimated at more than 90% and 46(3) μs [see Fig. 2 (bottom)]. The proposed level scheme of $^{115}$Mo with the tentatively assigned spins and parities is displayed in Fig. 3. The intensity of the 94-keV $\gamma$ line in the spectrum is divided and placed as a doublet to account for the energy of the 188-keV level [see Fig. 2 (bottom)]. The energy 10-keV transition between the 198-keV and 188-keV levels is too small to be observed with the current experimental setup. The relative intensities of transitions were displayed in Table II. The large isomeric ratio indicates the lower spin of 198-keV level compared to that of the ground state [36–38].

TABLE I. $\gamma$-ray relative intensities and B($\sigma\lambda$) values for transitions depopulating the isomeric state in $^{111}$Zr, $^{113}$Nb, $^{115}$Mo, assuming different multipolarities.

| | | $B(\sigma\lambda)$ (W.u.) | | | | |
|---|---|---|---|---|---|---|
| Nuclei | $E\gamma$ (keV) | $E1$ | $M1$ | $E2$ | $M2$ | $E3$ |
| $^{111}$Zr | 265 | $1.6^{+36}_{-7} \times 10^{-7}$ | $1.2^{+27}_{-5} \times 10^{-5}$ | $1.3^{+31}_{-5} \times 10^{-1}$ | $1.0^{+22}_{-4} \times 10$ | $1.6^{+37}_{-7} \times 10^{5}$ |
| $^{113}$Nb | 135 | $1.6^{+21}_{-6} \times 10^{-7}$ | $1.2^{+15}_{-5} \times 10^{-5}$ | $4.0^{+53}_{-15} \times 10^{-1}$ | $2.4^{+31}_{-9} \times 10$ | $7.4^{+98}_{-27} \times 10^{5}$ |
| $^{115}$Mo | 198 | $6.1^{+123}_{-24} \times 10^{-11}$ | $4.7^{+95}_{-19} \times 10^{-9}$ | $9.3^{+187}_{-37} \times 10^{-5}$ | $7.2^{+143}_{-29} \times 10^{-3}$ | $2.2^{+43}_{-9} \times 10^{2}$ |
| | 10 | $4.4(4) \times 10^{-7}$ | $1.6(1) \times 10^{-5}$ | $2.8(2) \times 10^{-1}$ | $2.8(2) \times 10$ | $8.1(9) \times 10^{5}$ |

TABLE II. $\gamma$ relative intensities observed in $^{115}$Mo.

| $E\gamma$ (keV) | $E_i$ (keV) | $E_f$ (keV) | Relative intensity |
|---|---|---|---|
| 198 | 198 | 0 | 9(6) |
| 188 | 188 | 0 | 100(6) |
| 94 | 188 | 94 | 2(1) |
| 94 | 94 | 0 | 2(1) |

## IV. SUMMARY

In summary, the isomeric states in $^{111}$Zr, $^{113}$Nb, $^{115}$Mo have been identified with the decent decay spectroscopy technique, which provides the first spectroscopy in the well-known nuclear region of prolate-to-oblate shape-phase transition. Future research is essential to study the shape transition in this region in detail by employing more direct experimental techniques, such as Coulomb excitation, charge radius measurements, etc.

## ACKNOWLEDGMENTS

This work was carried out at the RIBF operated by RIKEN Nishina Center and CNS, University of Tokyo. This research was sponsored in part by the Office of Nuclear Physics, U.S. Department of Energy under Awards No. DE-AC02-98CH10886 (BNL), No. DE-FG02-96ER40983 (UTK), and No. DE-AC05-00OR22725 (ORNL), and by the National Nuclear Security Administration under the Stewardship Science Academic Alliances program through DOE Award No. DE-NA0002132, by the National Science Foundation under Grants No. PHY-1430152 (JINA Center for the Evolution of the Elements), No. PHY-1565546 (NSCL), and No. PHY1714153 (Central Michigan University), by the Polish National Science Center under Contract No. UMO-2015/18/E/ST2/00217, by JSPS KAKENHI (Grants No. 14F04808, No. 17H06090, No. 25247045, No. 19340074, and No. 20H05648), by the UK Science and Technology Facilities Council ST/P005314/1, by NKFIH (NN128072), by the Janos Bolyai research fellowship of the Hungarian Academy of Sciences, by the UNKP-18-4-DE-449 New National Excellence Program of the Ministry of Human Capacities of Hungary, by Spanish Ministerio de Economia y Competitividad grants (No. FPA2017-83946-C2-1-P, No. FPA2011-28770-C03-03, No. FPA2014-52823-C2-1-P, No. FPA2014-52823-C2-2-P, No. FPA2014-57196-C5-4-P, No. FPA2017-84756-C4-2-P, No. SEV-2014-0398, and No. IJCI-2014-19172), by the Ministerio de Ciencia e Innovacion Grant No. PID2019-104714GB-C21, by European Commission FP7/EURATOM Contract No. 605203, by the H2020 Euratom SANDA project (Grant No. 847552), by the UK Nuclear Data Network funded by the UK Science and Technology Facilities Council Grant No. ST/N00244X/1, by the National Research Foundation (NRF) in South Korea (Grants No. 2016K1A3A7A09005575 and No. 2015H1A2A1030275), and by the Natural Sciences and Engineering Research Council of Canada (NSERC) via the Discovery Grants No. SAPIN-2014-00028 and No. RGPAS 462257-2014. Theoretical calculation in this Letter was supported by the National Natural Science Foundation of China under Grants No. 11835001 and No. 12035001.

[1] M. Goeppert Mayer, Nobel Lecture (1963).
[2] S. A. Johansson, Nucl. Phys. **64**, 147 (1965).
[3] T. Otsuka and Y. Tsunoda, J. Phys. G **43**, 024009 (2016).
[4] D. Arseniev, A. Sobiczewski, and V. Soloviev, Nucl. Phys. A **139**, 269 (1969).
[5] R. Sheline, I. Ragnarsson, and S. Nilsson, Phys. Lett. B **41**, 115 (1972).
[6] T. Sumikama, K. Yoshinaga, H. Watanabe, S. Nishimura, Y. Miyashita, K. Yamaguchi, K. Sugimoto, J. Chiba, Z. Li, H. Baba *et al.*, Phys. Rev. Lett. **106**, 202501 (2011).
[7] E. Cheifetz, R. C. Jared, S. G. Thompson, and J. B. Wilhelmy, Phys. Rev. Lett. **25**, 38 (1970).
[8] F. Browne, A. M. Bruce, T. Sumikama, I. Nishizuka, S. Nishimura, P. Doornenbal, G. Lorusso, P.-A. Söderström, H. Watanabe, R. Daido *et al.*, Phys. Lett. B **750**, 448 (2015).
[9] J. Ha, T. Sumikama, F. Browne, N. Hinohara, A. M. Bruce, S. Choi, I. Nishizuka, S. Nishimura, P. Doornenbal, G. Lorusso *et al.*, Phys. Rev. C **101**, 044311 (2020).
[10] F. R. Xu, P. M. Walker, and R. Wyss, Phys. Rev. C **65**, 021303(R) (2002).
[11] P. Möller, A. Sierk, T. Ichikawa, and H. Sagawa, At. Data Nucl. Data Tables **109-110**, 1 (2016).
[12] P. Kumar, V. Thakur, S. Thakur, V. Kumar, and S. K. Dhiman, Eur. Phys. J. A **57**, 36 (2021).
[13] J. P. Delaroche, M. Girod, J. Libert, H. Goutte, S. Hilaire, S. Péru, N. Pillet, and G. F. Bertsch, Phys. Rev. C **81**, 014303 (2010).
[14] N. Paul, A. Corsi, A. Obertelli, P. Doornenbal, G. Authelet, H. Baba, B. Bally, M. Bender, D. Calvet, F. Château *et al.*, Phys. Rev. Lett. **118**, 032501 (2017).
[15] L. Geng, H. Toki, S. Sugimoto, and J. Meng, Prog. Theor. Phys. **110**, 921 (2003).
[16] B. Sorgunlu and P. Van Isacker, Nucl. Phys. A **808**, 27 (2008).
[17] K.-L. Kratz, B. Pfeiffer, O. Arndt, S. Hennrich, A. Wöhr *et al.* (Collaborations), Eur. Phys. J. A **25**, 633 (2005).
[18] H. Watanabe, K. Yamaguchi, A. Odahara, T. Sumikama, S. Nishimura, K. Yoshinaga, Z. Li, Y. Miyashita, K. Sato, L. Pr.chniak *et al.*, Phys. Lett. B **704**, 270 (2011).
[19] G. Lorusso, S. Nishimura, Z. Y. Xu, A. Jungclaus, Y. Shimizu, G. S. Simpson, P.-A. Söderström, H. Watanabe, F. Browne, P. Doornenbal *et al.*, Phys. Rev. Lett. **114**, 192501 (2015).
[20] F. Montes, T. C. Beers, J. Cowan, T. Elliot, K. Farouqi, R. Gallino, M. Heil, K.-L. Kratz, B. Pfeiffer, M. Pignatari, and H. Schatz, Astrophys. J. **671**, 1685 (2007).
[21] N. Fukuda, T. Kubo, T. Ohnishi, N. Inabe, H. Takeda, D. Kameda, and H. Suzuki, Nucl. Instrum. Methods Phys. Res. Sect. B **317**, 323 (2013).

[22] S. Nishimura, G. Lorusso, Z. Xu, J. Wu, R. Gernhaüser, H. S. Jung, Y. K. Kwon, Z. Li, K. Steiger, and H. Sakurai, RIKEN Accel. Prog. Rep. **46**, 182 (2013).

[23] R. Yokoyama, M. Singh, R. Grzywacz, A. Keeler, T. T. King, J. Agramunt, N. T. Brewer, S. Go, J. Heideman, J. Liu *et al.*, Nucl. Instrum. Methods Phys. Res. Sect. A **937**, 93 (2019).

[24] A. Tolosa-Delgado, J. Agramunt, J. L. Tain, A. Algora, C. Domingo-Pardo, A. I. Morales, B. Rubio, A. Tarifeño-Saldivia, F. Calviño, G. Cortes *et al.*, Nucl. Instrum. Methods Phys. Res. Sect. A **925**, 133 (2019).

[25] A. Tarifeño-Saldivia, J. L. Tain, C. Domingo-Pardo, F. Calviño, G. Cortés, V. H. Phong, A. Riego, J. Agramunt, A. Algora, N. Brewer *et al.*, J. Inst. **12**, P04006 (2017).

[26] S. Nishimura, Prog. Theor. Exp. Phys. **2012**, 03C006 (2012).

[27] P.-A. Söderström, S. Nishimura, P. Doornenbal, G. Lorusso, T. Sumikama, H. Watanabe, Z. Y. Xu, H. Baba, F. Browne, S. Go *et al.*, Nucl. Instrum. Methods Phys. Res. Sect. B **317**, 649 (2013).

[28] J. Wu, S. Nishimura, G. Lorusso, Z.Y. Xu, H. Baba, F. Browne, R. Daido, P. Doornenbal, Y. F. Fang, E. Ideguchi *et al.*, AIP Conf. Proc. **1594**, 388 (2014).

[29] J. L. Tain, J. Agramunt, D. S. Ahn, A. Algora, J. M. Allmond, H. Baba, S. Bae, N. T. Brewer, R. Caballero Folch, F. Calvino *et al.*, Acta Phys. Pol. B **49**, 417 (2018).

[30] Z. Y. Xu, S. Nishimura, G. Lorusso, F. Browne, P. Doornenbal, G. Gey, H.-S. Jung, Z. Li, M. Niikura, and P.-A. Söderström, Phys. Rev. Lett. **113**, 032505 (2014).

[31] J. Wu, S. Nishimura, G. Lorusso, P. Möller, E. Ideguchi, P.-H. Regan, G. S. Simpson, P.-A. Söderström, P. M. Walker, H. Watanabe *et al.*, Phys. Rev. Lett. **118**, 072701 (2017).

[32] T. Kibédi, T. Burrows, M. Trzhaskovskaya, P. Davidson, and C. Nestor Jr., Nucl. Instrum. Methods Phys. Res. Sect. A **589**, 202 (2008).

[33] F. Kondev, M. Wang, W. Huang, S. Naimi, and G. Audi, Chin. Phys. C **45**, 030001 (2021).

[34] P. Möller and J. Nix, Nucl. Phys. A **536**, 20 (1992).

[35] P. Endt, At. Data Nucl. Data Tables **26**, 47 (1981).

[36] J. N. Wilson, D. Thisse, M. Lebois, N. Jovančević, D. Gjestvang, R. Canavan, M. Rudigier, D. Étasse, R-B. Gerst, L. Gaudefroy *et al.*, Nature (London) **590**, 566 (2021).

[37] M. Bowry, Zs. Podolya k, S. Pietri, J. Kurcewicz, M. Bunce, P. H. Regan, F. Farinon, H. Geissel, C. Nociforo, A. Prochazka *et al.*, Phys. Rev. C **88**, 024611 (2013).

[38] M. Bentaleb, E. Lubkiewicz, N. Schulz, J. L. Durell, F. Lidén, C. J. Pearson, W. R. Phillips, j. Shannon, B. J. Varley, C. J. Lister, I. Ahlnad, L. R. Morss, K. L. Nash, and C. W. Williams, Z. Phys. A **348**, 245 (1994).